Acta of Bioengineering and Biomechanics
Vol. 13, No. 3, 2011

Original paper

Material aspects of growth plate modelling using Carter's and Stokes's approaches

SZCZEPAN PISZCZATOWSKI*

Białystok University of Technology, Faculty of Mechanical Engineering, Poland.

Growth plate, named also as physis, is the anatomical structure responsible for the bone growth. Apart from numerous biological and biochemical factors, biomechanics has also strong influence on its functioning. Loadings acting on the bone element during its development can change (increase or decrease) the velocity of growth. This way mechanobiological processes influence the skeletal development.

Several theories try to describe the relationship between loadings acting on the physis and biological processes leading to bone growth and development. Unfortunately, some serious discrepancies exist between them. Additionally, difficulties occur during the modelling of the growth plate activity, which results from the problems in determining material parameters of the particular physis component.

The aim of the study was to analyse the influence of material properties of particular parts of the physis on biomechanical conditions of the bone growth. Two concepts, based on the Carter's and Stokes's approaches, were applied to estimate the biomechanical stimulation of the bone growth occurring within the physis volume.

Results of the numerical simulations show that due to inhomogeneity of the physis structure, the complex 3-D stress state occurs within the growth plate even in the case of uniform axial pressure acting on its surface. The value of the cartilage Poisson's ratio has a significant influence on the biomechanics of the growth plate activity estimated using both theories. Carter's model is additionally very sensitive to its dilatational parameter. Both methods lead to non-uniform patterns of mechanical stimulation of the bone growth within the volume of the cartilage. The differences in the stiffness between cartilaginous and bone parts of the growth plate are of fundamental importance for such phenomenon.

Key words: *growth plate, mechanobiology, modelling, cartilage*

1. Introduction

Growth plate, named also as physis, is the structure insulating metaphysis from epiphysis. It occurs in long bones throughout its development and is responsible for longitudinal bone growth [1]. Physis consists of three tissue types (figure 1a): the growth cartilage, the newly formed trabecular bone of the metaphysis and the fibrous tissue surrounding the cartilage (the ring of Lacroix). Chondrocytes occurring in the growth plate are crucial for bone development. They begin to divide in the proximal part of the physis (proliferating zone). More distally (hyperthropic zone), divided cells are separated from each other and their longitudinal size increases. The growth of cartilage inside the physis is continuous, but the growth plate does not become thicker. Cartilage is, however, still resorbed and turned into bone at the metaphyseal side (the zone of calcification). This way, cartilage growth leads to diaphysis elongation.

Longitudinal growth inside the physis depends on both proliferation and hyperthrophy of chondrocytes [2]. Apart from numerous biological and biochemical factors (hormones activity, local growth factors, etc.), mechanical loadings have great influence on these

* Corresponding author: Szczepan Piszczatowski, Faculty of Mechanical Engineering, Białystok University of Technology, Wiejska 45c, 15-351 Białystok, Poland. Tel: +4885 746-92-54, fax: +4885 746-92-48, e-mail: spisz@pb.edu.pl

Received: February 20th, 2011
Accepted for publication: June 14th, 2011

processes [3], [4]. It is a well-known fact that forces acting on the bone element can change, increase or decrease the velocity of its growth. This way, mechanobiological phenomenon can influence the skeletal growth and development.

The Hueter–Volkmann law, formulated as early as in the 19th century but still frequently used in medical literature, assumes that increased pressure acting on the growth plate retards bone growth and conversely, reduced pressure or even tension accelerates it [5]–[7]. More recently, the Hueter–Volkmann law was the basis for STOKES's research [3], [8]–[10]. Based on the experiments with the use of animal cartilage, he stated that endochondral growth rate is proportional to the value of longitudinal stresses acting on the growth plate: an increase of the compressive stresses retards growth, whilst tension accelerates it. It must be noticed, however, that in experiments performed by Stokes, the role of axial loadings was predominant (e.g., vertebral bone). Loadings were always applied in continuous manner. More complex analysis of the mechanical influences on the bone growth was presented by FROST [11]. He proposed the "Chondral Growth–Force Response Characteristics" (CGFRC), where the mechanical stimulation of the bone growth was dependent not only on the sense of stresses but also on their value. For stresses not exceeding the physiological range, the endochondral growth runs faster in the case of compression compared to tension. Similar conclusions were proposed also by PAUWELS [12]. He stated that in the growth plate subjected to bending, growth runs faster on the compressed site compared to the traction site. However, in the Frost theory, compression exceeding physiological range slows down or even inhibits growth.

All the theories presented above assume uniaxial stress state (tension–compression) within the growth plate. Most real anatomical situations are much more complex, and three-dimensional stress and strain analysis should be considered. Such an approach was proposed by CARTER in his theory firstly assigned to the modelling of the cartilage ossification. It was assumed that hydrostatic pressure maintains cartilage while shear or tensile stresses damage it and promote cartilage growth and ossification [13]–[15]. Similar formula to analyse the bone growth velocity was proposed by STEVENS et al. [16].

A more detailed comparison of all the theories presented above leads to a surprising conclusion – there are many discrepancies between particular conceptions despite the fact that all authors have presented abundant clinical evidence corresponding to their theories. It seems that insufficiently detailed analysis of the particular clinical cases and excessive generalization of the results obtained are the main problems.

It should be noticed that there are some attempts to carry out much more complex analysis of the growth cartilage and bone tissue, using nonlinear biphasic, poroelastic or viscoelastic models [17]–[20]. However, such methods are much more difficult to use in practice when the development of real anatomical objects is analysed. For this reason, a single-phase elastic model is still very attractive, but its further analysis is necessary, especially in order to understand the influence of the three-dimensional stress state in conjunction with material properties of the cartilage and surrounding tissues (epiphysis, metaphysis, the ring of Lacroix).

Numerical simulations presented in this paper were focused on a better understanding of the biomechanics of the growth plate. Special attention was paid to the influence of particular material parameters applied in the model on the stress and strain patterns occurring in the cartilage. Carter's and Stokes's approaches were used to evaluate the biomechanical stimulation of the bone growth. A comparison of these methods was one of the crucial aims of this study. All analyses were made using single-phase, elastic model of the cartilage. Further analyses, taking into account other loading conditions as well as the geometrical aspects of the growth plate structure, will be presented in the following part of the studies.

2. Methods

Numerical simulations with the use of the finite element methods constituted the main tool applied in the research. The modelling process as well as numerical analyses were performed using ANSYS package (*Ansys. Inc.*).

2.1. Geometrical and material model of the growth plate

Idealized, very simplified model of the growth plate was prepared for numerical analyses of the physis. A flattened cylinder composed of the growth cartilage was its main part (figure 1b). A thin layer of trabecular bone was added above the cartilage to model the bone plate occurring at the distal end of epiphysis. At the bottom of the cartilage, a trabecular metaphysis was modelled. The ring of Lacroix was

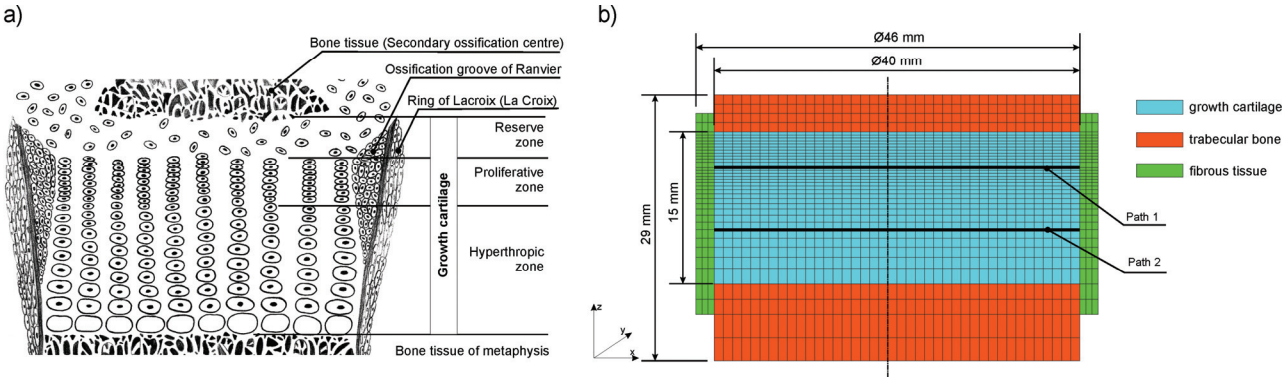

Fig. 1. Growth plate: a) anatomical scheme, b) cross-section of the geometrical model used in FEM analysis (Path 1 and Path 2 – lines used during post-processor analyses)

placed around the whole growth cartilage and partly around the bone plates. A finite element model was made with the use of 3D 20-node structural elements (SOLID186). Particular parts of the model were strictly connected to each other on its common nodes.

All tissues were treated as a linearly elastic, isotropic material. Dissimilar information about mechanical properties of the growth cartilage is presented in the literature [10], [13], [14], [16], [21]–[24]. It is possible to find the value of axial elastic modulus in the range from 0.2 MPa [18] to 23.8 MPa and even 1157 MPa [19]. Poisson's coefficient is also taken in a wide range. VILLEMURE and STOKES [10], using transversely isotropic model, present $\nu_{31} \leq 0.1$ for out-of-plane Poisson's ratio and $\nu_{21} = 0.24$–0.3 for transverse Poisson's ratio. LIN et al. [22] used in the numerical simulations $\nu = 0.12$ for growing and mineralized area, whilst $\nu = 0.4$ for loading sensitive area, RIBBLE et al. [24] used $\nu = 0.4$ for the whole growth plate, whilst SYLVESTRE et al. [21] used $\nu = 0.49$. CARTER and WONG [15] stated that Poisson's ratio should be slightly less than 0.5 or equal to it (incompressible material). Using displacement-based finite element formulation, they used $\nu = 0.47$ [13], but in later analyses with hybrid elements, Poisson's ratio was increased to $\nu = 0.49$ [23], [25], [26].

In the present analyses, based mainly on the CARTER's research [13], [25], [26], in the primary model of the growth cartilage, the following material properties were taken: elastic modulus $E_{GC} = 6$ MPa, Poisson's coefficient $\nu_{GC} = 0.495$ (table 1, model No. 6). Cartilage was treated as an almost incompressible material, and for this reason, analyses were performed using the mixed u–P formulation [27]. In order to evaluate the role of mechanical properties in other variants of the model, various values of material pa-

Table 1. Material properties of growth plate model

Variant No.	Growth cartilage		Trabecular bone		Fibrous tissue (ring of Lacroix)	
	Elastic modulus E_{GC} (MPa)	Poisson's coefficient (–)	Elastic modulus E_B (MPa)	Poisson's coefficient (–)	Elastic modulus E_F (MPa)	Poisson's coefficient (–)
1	6	0.3	345	0.3	10	0.3
2	6	0.4	345	0.3	10	0.3
3	6	0.45	345	0.3	10	0.3
4	6	0.47	345	0.3	10	0.3
5	6	0.49	345	0.3	10	0.3
6	6	0.495	345	0.3	10	0.3
7	6	0.4999	345	0.3	10	0.3
8	6	0.495	345	0.495	10	0.495
9	6	0.495	100	0.3	10	0.3
10	6	0.495	20	0.3	10	0.3
11	6	0.495	6/20*	0.3	10	0.3
12	6	0.495	345	0.3	0.1	0.3
13	6	0.495	345	0.3	100	0.3

* 6 MPa – proximal bone plate; 20 MPa – distal bone plate.

rameters were considered (table 1). It must be emphasised that the value of some parameters was intentionally exaggerated in some cases. Such a stratagem was used only to magnify the effect observed. Special attention was paid to Poisson's coefficient in growth cartilage. This parameter, however, can strongly influence the 3D stress and strain patterns occurring in an inhomogeneous structure. Seven values, in the range from 0.3 to 0.4999, were analysed. Various parameters of the tissues surrounding the growth cartilage were modelled as well. Poisson's coefficients of the trabecular bone (ν_B) and fibrous tissue (ν_F) were equal $\nu_B = \nu_F = 0.3$ besides the variant No. 8, where $\nu_B = \nu_F = 0.495$ was taken to simulate the situation where the values of Poisson's coefficient are identical for all materials. Four variants of the trabecular bone elastic modulus (E_B) were analysed. The basal value was $E_B = 345$ MPa [24]. Simulation of the less rigid bone plates was performed using successively $E_B = 100$ MPa and $E_B = 20$ MPa. The most flexible bone tissues were analysed in the model No. 11 where the Young modulus for the distal plate was equal to 20 MPa, whilst for proximal plate – 6 MPa (similar to that of growth cartilage). Three variants of the fibrous ring of Lacroix were simulated. The basal value of the elastic modulus was $E_F = 10$ MPa. The negligible meaning of the fibrous ring was assumed in model No. 12 ($E_F = 0.1$ MPa), whilst much stiffer fibrous ring was taken in model No. 13 ($E_F = 100$ MPa). All the variants of the material model were compared in table 1.

2.2. Loadings and constraints

The model was fully constrained on its distal nodes, which reflects ideal connection of the growth plate with metaphysis. Loadings were applied on the proximal bone plate using a uniform surface pressure. Resultant value of the loads applied (200 N) was taken arbitrarily. It seems, however, that similar value of compressive forces could appear in the small children's femur or tibia.

2.3. Analysis of the mechanical stimulation of endochondral growth

Stress and strain patterns were calculated for particular variants of the material model. For all elements representing the cartilage, the "growth index" (GI) expressing the intensity of mechanical stimulation of the endochondral bone growth was calculated using:

a) the Carter's approach [13]:

$$GI_1 = \sigma_S + a\sigma_H \ (\mathrm{N/m^2}), \tag{1}$$

where:

σ_S – octahedral shear stress (always positive, increases the value of the GI_1, accelerates cartilage ossification and growth),

σ_H – hydrostatic stress (negative in compression and positive in tension),

a – weighting factor (dilatational parameter);

b) the Stokes's approach [8]:

$$GI_2 = \sigma_z \ (\mathrm{N/m^2}), \tag{2}$$

where σ_z stands for axial stress.

The value of the dilatational parameter a in formula (1) was tested by CARTER and WONG in the range of 0.1–2 with the final suggestion that the most suitable for diarthroidal joints development is $a = 0.5$ [13]. It is obvious that greater values of a increase the importance of the compressive hydrostatic stresses (the inhibition of ossification and growth) compared to the octahedral shear stresses (the acceleration of ossification and growth). WONG and CARTER [15] used $a = 0.18$, STEVENS et al. [16] used $a = 0.35$ (combination with the minimum of the hydrostatic stresses calculated for complete loading cycle) and WONG and CARTER [28] made use of $a = 0.7$. However, the value of the weighting factor most frequently is taken as equal to 0.5. In the present research, twelve values of the coefficient a were tested in the range of 0.1–2 (0.1; 0.2; 0.3; 0.4; 0.5; 0.6; 0.7; 0.8; 1.0; 1.3; 1.7; 2.0).

The patterns of the "growth indexes" were plotted for the axial cross-section of the growth plate. Additionally, two paths were defined: the first (Path 1) was passing through the proximal part of the growth cartilage (proliferative zone), the second (Path 2) was drawn more distally, through the hyperthropic zone (figure 1b).

3. Results

The patterns of the hydrostatic stresses and octahedral shear stresses, calculated within the growth cartilage using primary material model (No. 6) loaded with uniform, symmetric axial compression, were presented in figure 2. Two important remarks can be made very easily: (1) even for uniform axial loading, the complex 3-D stress state is obtained within the structure of the growth plate as a result of its inhomogeneity, (2) due to essential dissimilarities between the hydrostatic and octahedral shear stress patterns,

the growth index GI_1 (being the weighted sum of both of them), must be strongly dependent on the value of the weighting factor a (see formula (1)).

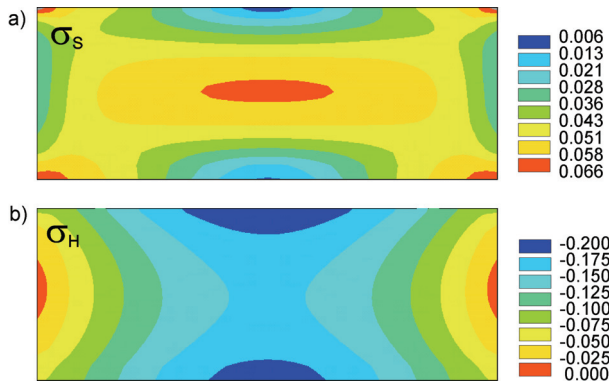

Fig. 2. Patterns of octahedral shear stresses σ_S (a) and hydrostatic stresses σ_H (b) calculated for material model No. 6 (see table 1). View on the axial cross-section of the growth cartilage; bone and fibrous parts of the model were omitted

The last statement is corroborated by several patterns of the index GI_1, calculated for the same model (model No. 6) but using different values of a and plotted in figure 3 (view on the axial cross-section) and figure 4 (for Path 1 and Path 2 trajectories). It is possible to observe that an increase of the coefficient a value leads to a decrease of the GI_1 in the central part of the growth cartilage. This is the effect of a growing importance of the compressive (negative value) hydrostatic stresses. The growth index GI_2 (axial compressive stresses) patterns were added in figure 4 for comparison.

Changes of the Poisson's coefficient of cartilage have influence on the three-dimensional deformity of the inhomogeneous structure of the growth plate and, in consequence, on the patterns of the hydrostatic and shear stresses. It is obvious that the pattern of the growth index GI_1 also depends on Poisson's ratio of the cartilage. The results obtained for different values

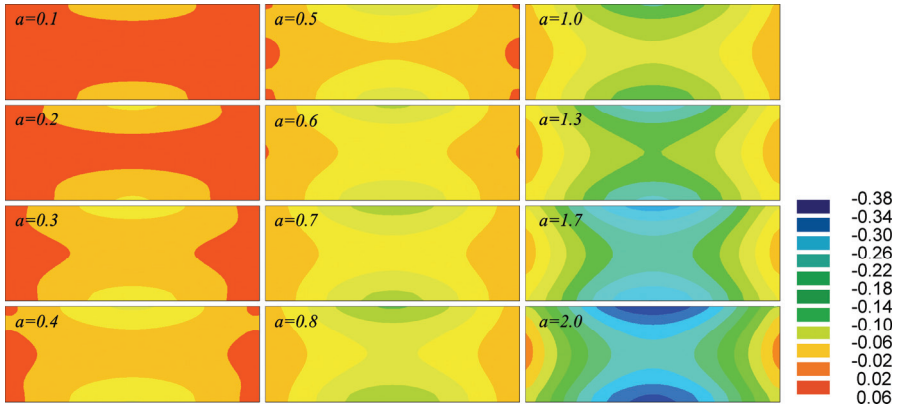

Fig. 3. Patterns of the growth index GI_1 calculated for material model No. 6 using different values of the weighting factor (dilatational parameter) a (view on the axial cross-section of the growth cartilage; bone and fibrous parts of the model were omitted)

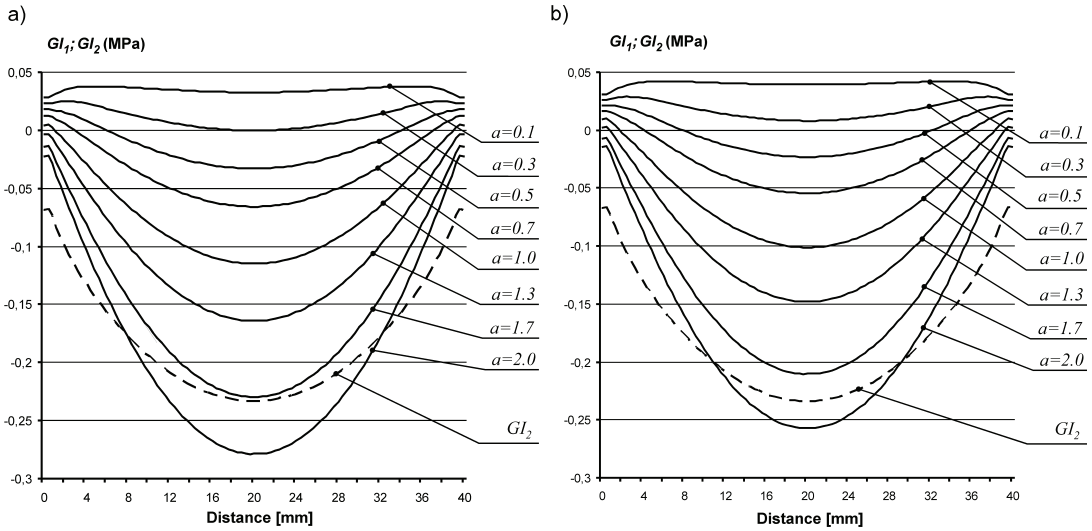

Fig. 4. Patterns of the growth index GI_1 calculated for material model No. 6 using different values of the weighting factor (dilatational parameter) a: a) inside the proliferative zone – Path P1, b) inside the hyperthropic zone – Path P2. Patterns of the growth index GI_2 added for comparison

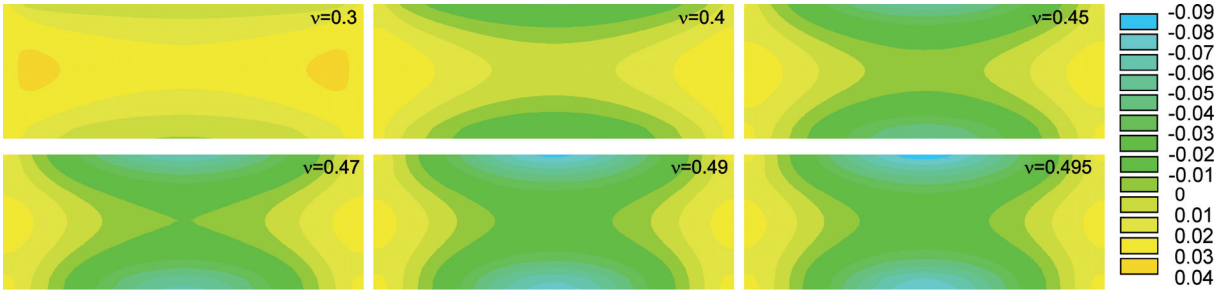

Fig. 5. Patterns of the growth index GI_1 calculated for different values of Poisson's coefficient of the cartilage for the weighting factor a = 0.5 (view on the axial cross-section of the growth cartilage)

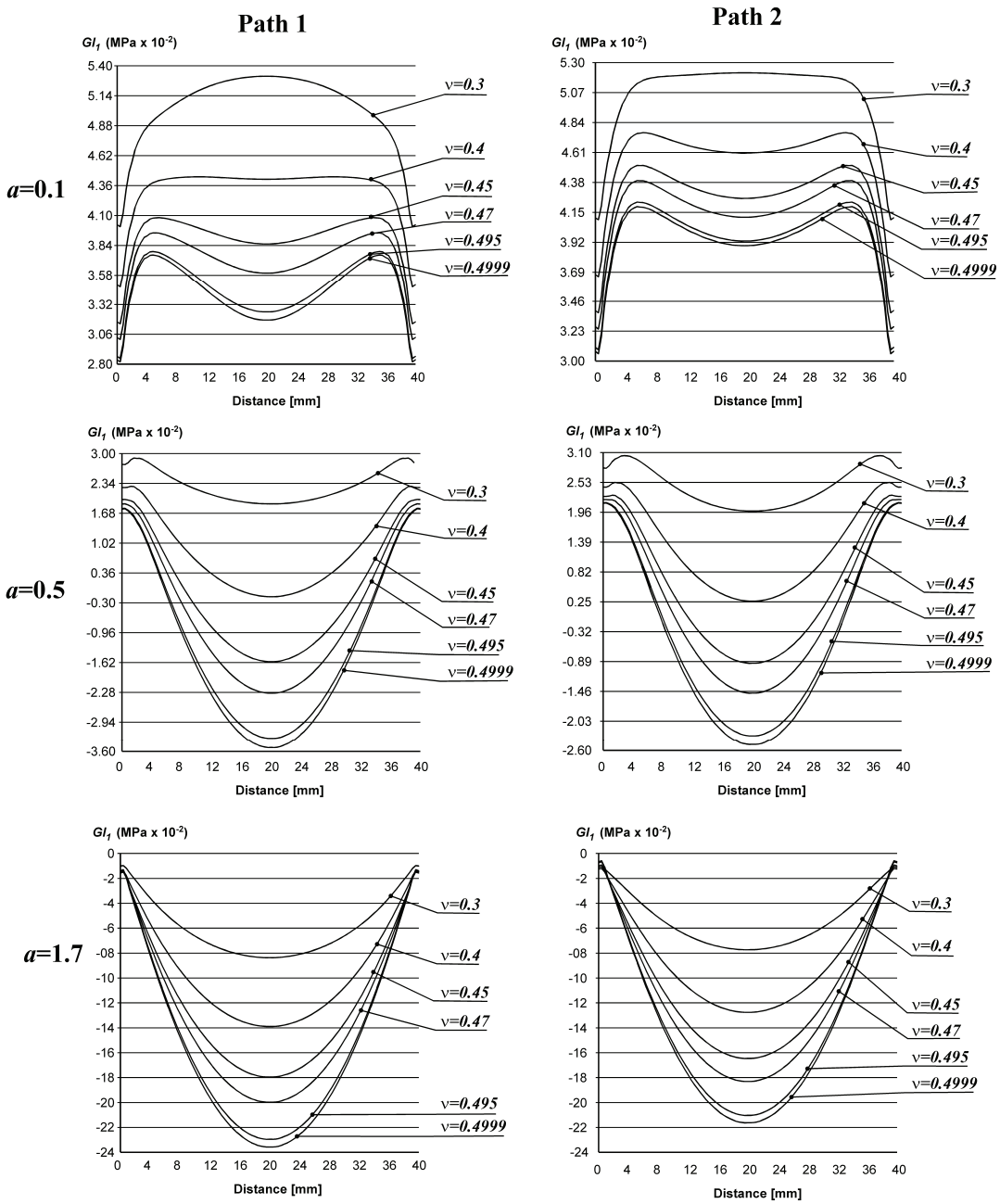

Fig. 6. Patterns of the growth index GI_1 calculated for different values of Poisson's coefficient of the cartilage and for the weighting factor a = 0.1, 0.5 and 2.0 inside the proliferative zone – Path 1 and the hyperthropic zone – Path 2

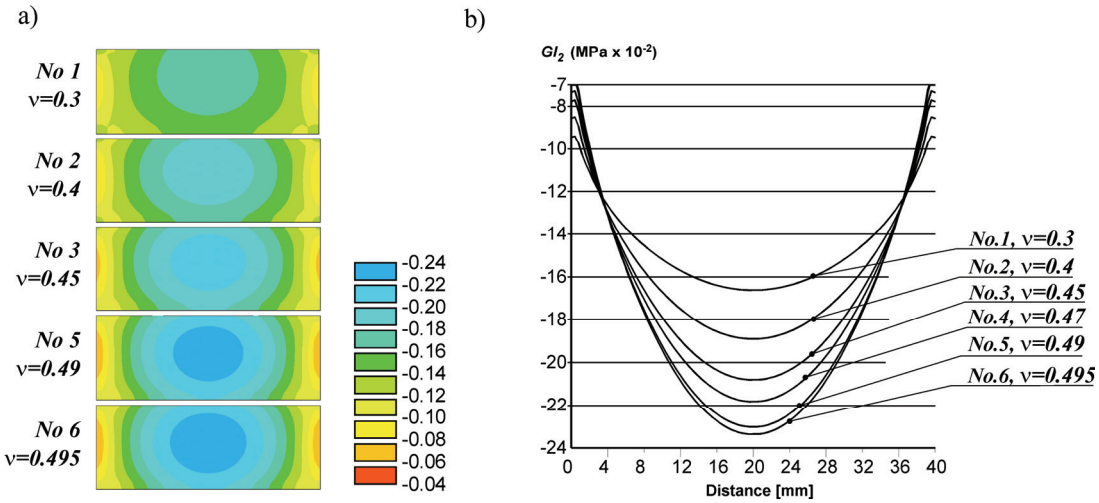

Fig. 7. Comparison of the patterns of the growth index GI_2 calculated for different values of Poisson's coefficient of the cartilage: a) inside proliferative zone – Path P1, b) inside hyperthropic zone – Path P2

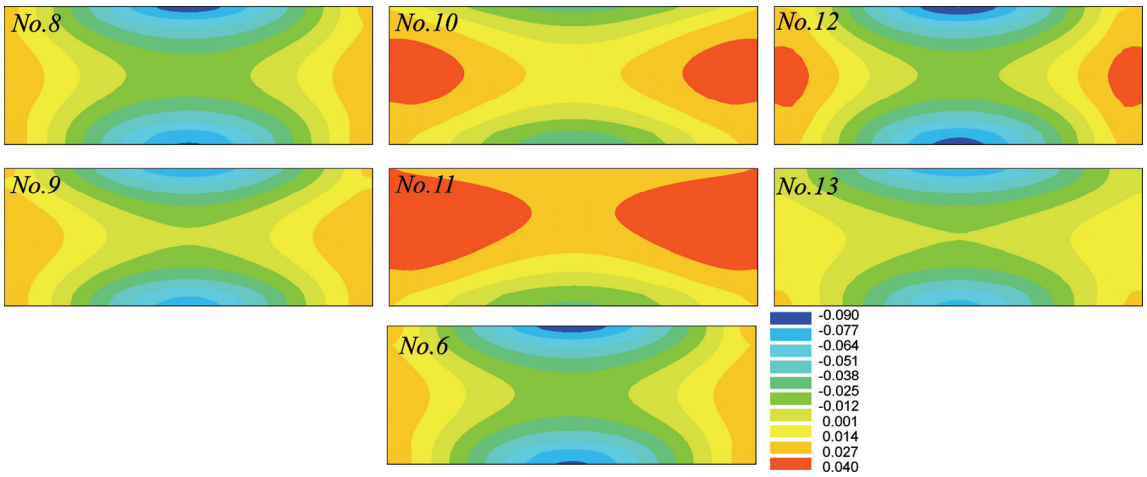

Fig. 8. Growth index GI_1 patterns calculated for different surroundings of the growth cartilage (view on the axial cross-section of the growth cartilage). More detailed description of particular models can be found in table 1

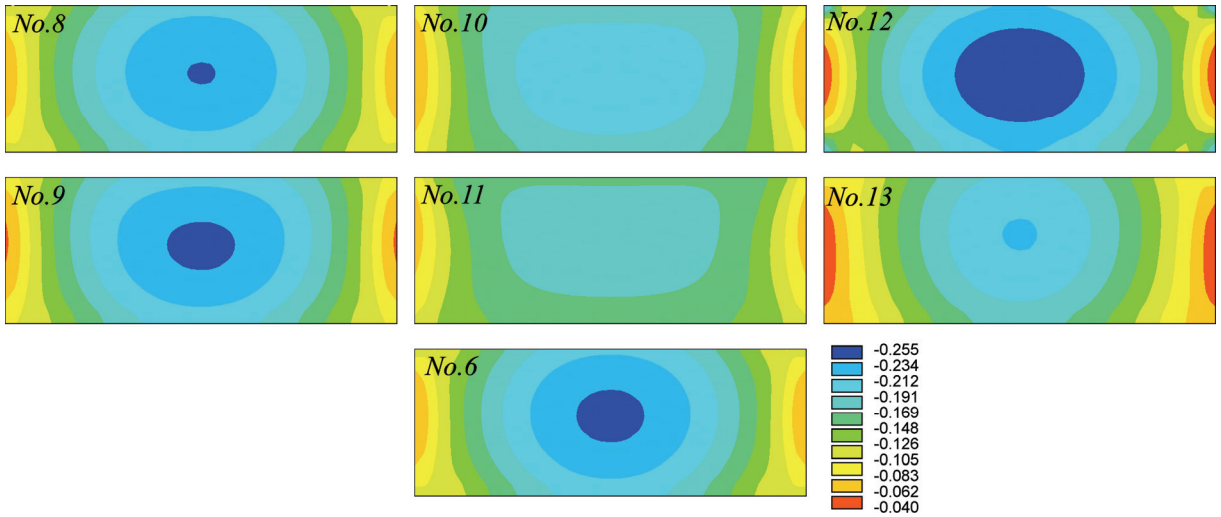

Fig. 9. Growth index GI_2 patterns calculated for different surroundings of the growth cartilage (view on the axial cross-section of the growth cartilage). More detailed description of particular models can be found in table 1

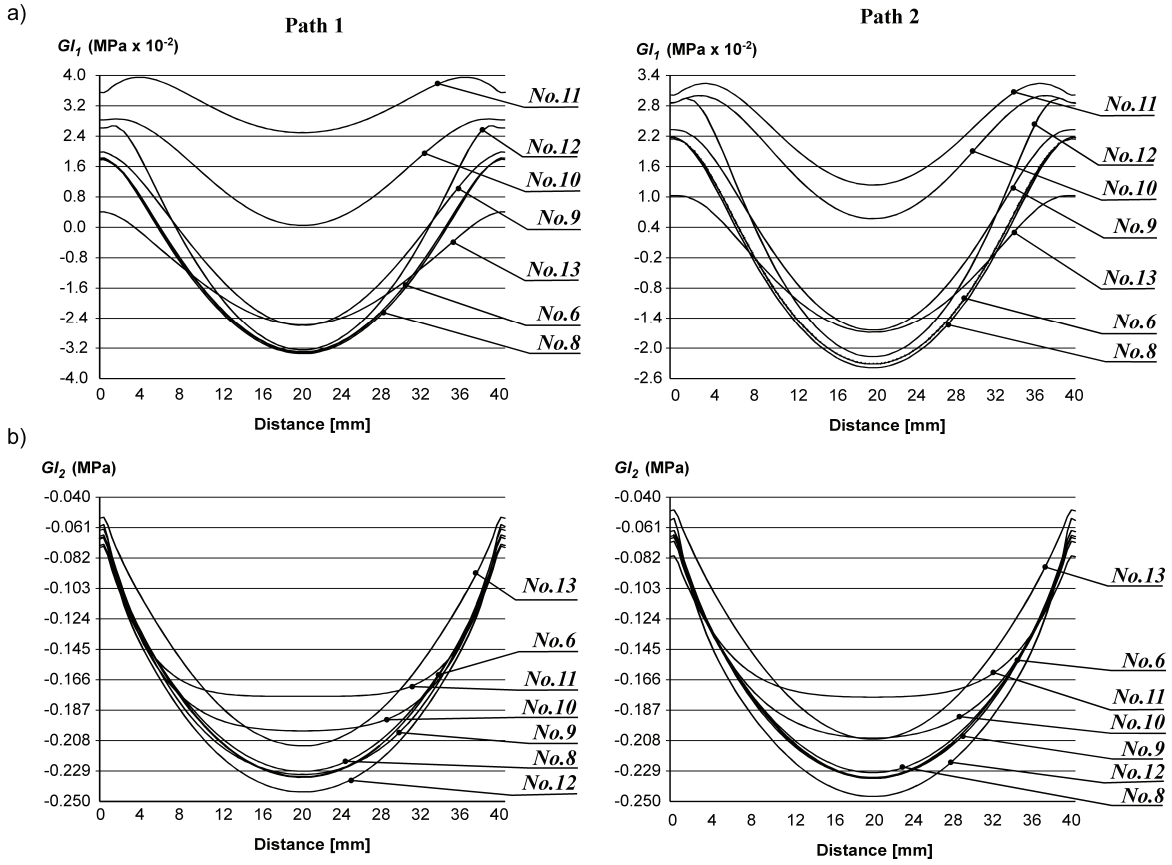

Fig. 10. Comparison of the growth index GI_1 (a) calculated for the weighting factor $a = 0.5$ and the growth index GI_2 (b) obtained for different surroundings of the growth cartilage. Plots made for Path 1 and Path 2. More detailed description of particular models can be found in table 1

of Poisson's coefficient of the cartilage were presented in figure 5. It can be seen that an increase of Poisson's ratio value results in a decrease of the index GI_1 in the central part of growth plate. Changes of the index GI_1 pattern resulting from the variety of Poisson's coefficient of the cartilage could interfere with the effects caused by an increase or a decrease of the value of the weighting factor a. The patterns obtained using $a = 0.5$ were presented in figure 5 (view on the axial cross-section) and in the central part of fig. 6 (for Path 1 and Path 2 trajectories). For comparison, analogous results calculated for Paths 1 and 2 were presented also for $a = 0.1$ and 2.0 (figure 6).

Using the lowest value of dilatational coefficient ($a = 0.1$), the shape of the curves representing GI_1 is more complex compared to those obtained for higher values of the parameter a. For the lowest values of both a and Poisson's coefficient the of cartilage it is possible to obtain the convex curves representing GI_1 along Path 1 and Path 2 in their central parts in contrast to majority of other cases, where curves are concave.

The patterns of the growth index GI_2 obtained using Stokes's approach were presented in figure 7a. Due to striking similarities of the plots obtained for both Path 1 and Path 2 lines, the curves representing the GI_2 were drawn only for the hyperthropic zone – Path 2 (figure 7b).

The influence of the different surroundings of growth cartilage on the biomechanical conditions within the cartilage was analysed using models No. 8–No. 13 (table 1). Appropriate patterns of growth indexes GI_1 and GI_2 were presented in figures 8, 9 and 10. The results calculated for the primary material model (No. 6) were added for comparison.

4. Discussion and conclusions

The first remark made based on the results presented above concerns the non-uniformity of mechanical stimulation of the growth cartilage within its volume, despite uniform axial loading acting on the growth plate. This result is clearly visible when both approaches, i.e. Carter's (index GI_1) and Stokes's (index GI_2), are compared. The source of

such phenomenon is the complex 3-D stress state occurring in the inhomogeneous structure of the growth plate, even in the case of the uniform axial loadings. The analysis of the results obtained for various material parameters of the growth cartilage surroundings shows that the difference in the values of elastic modulus between cartilage and trabecular bone plates located distally and proximally to the growing zone is of a fundamental importance (figures 8–10). On the other hand, the difference in the stiffness between these two types of tissue is indisputable because it results directly from cartilage calcification leading to bone formation. The fibrous ring surrounding the cartilage also seems to be quite important. Simulating very low stiffness of the fibrous tissue (model No. 12), some amplification of the inequality of GI_1 and GI_2 patterns was observed, whilst very high stiffness (model No. 13) made this effect much less intensive (figure 10). There was no effect of the changes of fibrous ring and Poisson's coefficients of bone tissue (model No. 8).

Non-uniformity of strain distribution within cartilaginous growth plate was earlier confirmed experimentally by VILLEMURE et al. [29]. Different patterns of the strain were recorded for reserve, proliferative and hypertrophic zones. One of the effects observed was even the appearance of the tensile strain in some parts of the cartilage, despite the compressive loading acting on the growth plate. This research confirms the importance of growth plate inhomogeneity, though the authors' attention was focused rather on the inner structure of the growth cartilage, while neglecting the role of the bone plates and the fibrous ring. Obviously, taking into account the differences in mechanical properties occurring between particular morphological zones of the growth cartilage, it would be possible to observe further non-uniformity of the stress pattern with all consequences for GI_1 and GI_2 indexes. Such an attempt should be considered in the future research.

It is meaningful that Carter's approach was used earlier to predict the velocity of bone growth only for very young children, when the whole cartilaginous epiphysis was modelled [23], [25], [26]. In such a situation, the lack of the proximal bone plate has a great influence on the effects of the simulation. RIBBLE et al. [24] placed the growth cartilage between two bone plates, but only shear stresses were analysed, while neglecting the hydrostatic component. LIN et al. [22] used a special layer of the element called "loading sensitive area" placed at the top of the growth plate. Loadings were applied directly on this layer and the stress state, calculated inside

Table 2. Correlation coefficients between the sets of GI_1 and GI_2 values calculated for Path 1 and Path 2 using different material models and different values of dilatational parameter a

a	Path No.	Material model No.						
		1	2	3	4	5	6	7
0.1	1	–0.974	–0.815	–0.491	–0.277	–0.034	0.028	0.088
	2	–0.893	–0.696	–0.568	–0.525	–0.494	–0.488	–0.484
0.2	1	–0.884	0.398	0.756	0.815	0.857	0.866	0.874
	2	–0.618	0.280	0.585	0.669	0.742	0.759	0.776
0.3	1	0.037	0.891	0.934	0.944	0.952	0.954	0.956
	2	0.232	0.808	0.888	0.910	0.930	0.935	0.940
0.4	1	0.851	0.956	0.968	0.972	0.975	0.976	0.977
	2	0.748	0.918	0.948	0.958	0.967	0.968	0.971
0.5	1	0.947	0.975	0.980	0.982	0.984	0.984	0.985
	2	0.885	0.952	0.968	0.974	0.979	0.980	0.982
0.6	1	0.971	0.983	0.986	0.987	0.988	0.989	0.989
	2	0.933	0.968	0.978	0.982	0.985	0.986	0.987
0.7	1	0.981	0.987	0.989	0.990	0.991	0.991	0.991
	2	0.954	0.976	0.983	0.986	0.989	0.989	0.990
0.8	1	0.986	0.990	0.991	0.992	0.993	0.993	0.993
	2	0.966	0.981	0.987	0.989	0.991	0.991	0.992
1.0	1	0.991	0.992	0.993	0.994	0.994	0.995	0.995
	2	0.978	0.987	0.990	0.992	0.993	0.993	0.994
1.3	1	0.994	0.995	0.995	0.996	0.996	0.996	0.996
	2	0.985	0.991	0.993	0.994	0.995	0.995	0.996
1.7	1	0.995	0.996	0.996	0.997	0.997	0.997	0.997
	2	0.990	0.993	0.995	0.996	0.996	0.996	0.997
2.0	1	0.996	0.996	0.997	0.997	0.997	0.997	0.997
	2	0.991	0.994	0.995	0.996	0.997	0.997	0.997

these elements, was used to estimate the mechanical stimulation of the more distally located "growth area". All the examples mentioned above could confirm the tendency to neglect the non-uniformity of the mechanical stimulation of the growth cartilage located between trabecular epiphysis and metaphysis when Carter's approach is used.

Growth index calculated using Carter's concept greatly depends on the value of the dilatational parameter a (formula (1)) used to establish relations between hydrostatic and octahedral shear stresses (figures 3 and 4). Different values of this parameter can lead to antithetical conclusions. The same part of the growth plate for a certain value of the coefficient a can be more stimulated than surroundings and grow faster, whilst for the other value, it can be less stimulated than surroundings and grow slower. This effect became much more intensive when the influence of the dilatational parameter was combined with changes caused by Poisson's coefficient of the cartilage. Such an observation is very important because it helps realise that by manipulating the parameters of Carter's model it is possible to obtain contradictory results of the analysis. Further research is necessary to find rationale for the choice of the proper value of the coefficient a. The fact that CARTER and co-workers used different values of this parameter for various analyses [13], 15], [16], [28] confirms that the problem exists rather than helps solve it. The analyses of the mechanical influences on the chondrocytes performed on the cell level could be helpful in solving this problem in the future [30], [31], [32].

It must be noticed that both GI_1 and GI_2 indexes try to describe the same phenomenon (mechanical stimulation of the endochondral growth). It is obvious that both methods, if they are used in the same biomechanical situations, should bring about similar effects. In order to compare both attempts, correlation coefficients for particular sets of GI_1 and GI_2, calculated along the Paths 1 and 2, were determined for different material models and for different values of the dilatational parameter a (table 2).

Relatively low or even inverse correlation was obtained for $a \leq 0.4$. The higher values of a in Carter's model give better correlation with Stokes's approach. Higher values of Poisson's coefficient of cartilage enhance the correlation between both attempts. It is possible to observe that for $a \geq 0.5$ Carter's and Stokes's approaches give quite similar results for axial and symmetric loading. Taking into account not only correlation coefficients, but also the range of GI_1 and GI_2 values (figure 4), it seems that the greatest similarity between both indexes is revealed for $a = 1.7$. Such an observation corresponds closely to the research presented by LIN et al. [22]. They stated that at $a = 0.5$ Carter's model presents weak ability to simulate growth retardation resulting from compressive loadings. A higher value of a (for example, $a = 1.7$) leads, however, to amplification of the role of negative hydrostatic stresses.

The value of the Poisson's coefficient of the cartilage seems to be crucial for the evaluation of the mechanobiological influences on the growth plate activity. It is common for Carter's and Stokes's approaches. This fact shows once again that the understanding of 3-D deformities occurring in the cartilage is necessary for effective analyses of the growth plate mechanobiology. On the other hand, the great influence of Poisson's coefficient of the cartilage indicates the risk of growth disturbances in the case of any changes in the internal structure of the cartilage. It is, however, very probable that Poisson's ratio of cartilage can change as a result of disturbances of such parameters as water content. The measurement of Poisson's coefficient for the growth cartilage is difficult and usually an approximate value is used in numerical analyses. The present results testify to the risk of serious mistakes of mechanobiological analyses performed with the use of unrealistic material properties.

To conclude, it should be noticed that STOKES [8] in his original theory based on the Hueter–Volkmann principle has neglected the non-uniformity of the axial stresses in the growth plate resulting from its inhomogeneity. If the velocity of the bone growth was linearly dependent on the axial stresses – following the Stokes's concept – in view of the results obtained in the present research, bone, under uniform compression, should grow slower in its central part and faster in the periphery. However, apart from the material aspect, the geometry of the growth plate (shape, relation between height and diameter) may be very important. Carter's approach, as it was presented above, for some parameters gives the results very close to Stokes's method, but in reality is much more sophisticated. This theory, however, was originally based on the principle that loadings acting on the growth plate are variable. STEVENS et al. [16], using them to model endochondral growth, have assumed that mechanobiological contribution to the rate of cartilage maturation, and as a result to the velocity of bone growth, is dependent on the maximum value of the octahedral shear stress and the minimum value of the hydrostatic stress occurring during a complete loading cycle. However, in the case of cyclically acting axial compressive loading,

the maximum value of octahedral shear stress and the minimum value of hydrostatic stress are equal to those occurring under static axial compression. As a result, the velocity of growth generated in the cartilage loaded with uniform axial compressive loading, in view of Carter's theory, could be non-uniform within the volume of growth plate and strongly dependent on Poisson's coefficient of the cartilage as well as on the dilatational parameter. Obviously, the present conclusions should be verified for a different geometry of the growth plate, like in the case of the Stokes's theory.

A better understanding of the phenomenon considered in the present research gives a chance to elucidate some discrepancies occurring between the theories formulated by Hueter and Volkman, Frost, Pauwels, Stokes and Carter in the range of mechanobiological stimulation of bone growth. In this way, the analysis of the bone deformity occurring in numerous diseases, such as cerebral palsy [4], will be possible.

Acknowledgements

The author acknowledges financial support from the Ministry of Science and Higher Education (Poland), grant No. N518 043 32/3352.

References

[1] OGDEN J.A., *Anatomy and Physiology of Skeletal Development*, [in:] *Skeletal injury in the child*, Springer, New York, 2000.

[2] BALLOCK R.T., O'KEEFE R.J., *The biology of the growth plate*, J. Bone Joint Surg., 2003, 85-A, 715–726.

[3] STOKES I.A.F., *Mechanical effects on skeletal growth*, J. Musculoskel. Neuron. Interac., 2002, 2, 277–280.

[4] PISZCZATOWSKI S., *Analysis of the stress and strain in hip joint of the children with adductors spasticity due to cerebral palsy*, Acta Bioeng. Biomech., 2008, 10, 52–56.

[5] HUETER C., *Anatomische Studien an den Extremitaetengelenken Neugeborener und Erwachsener*, Virkows Archiv. Path. Anat. Physiol., 1862, 25, 572–599.

[6] VOLKMANN R., *Verletzungen und Kankenheiten der Bewegungsorgane*, [in:] von Pitha F.R., Billroth T., *Handbuch der allgemeinen und speciellen Chirurgie Bd UU*, Teil II, Ferdinand Enke, Stuttgart, 1882.

[7] MEHLMAN C.T., ARAGHI A., ROY D.R., *Hyphenated history: the Hueter–Volkmann law*, Am. J. Orthop., 1997, 26, 798–800

[8] STOKES I.A.F., ARONSSON D.D., DIMOCK A.N., CORTRIGHT V., BECK S., *Endochondral growth in growth plates of three species at two anatomical locations modulated by mechanical compression and tension*, J. Orthop. Res., 2006, 24, 1327–1334.

[9] STOKES I.A.F., CLARK K.C., FARNUM C.E., ARONSSON D.D., *Alternations in the growth plate associated with growth modulation by sustained compression or distraction*, Bone, 2007, 41, 197–205.

[10] VILLEMURE I., STOKES I.A.F., *Growth plate mechanics and mechanobiology. A survey of present understanding*, J. Biomech., 2009, 42, 1793–1803.

[11] FROST H.M., *A chondral modeling theory*, Calcif. Tissue Int., 1979, 28, 181–200.

[12] PAUWELS F., *Biomechanics of the Locomotor Apparatus*, Springer-Verlag, Berlin, 1980.

[13] CARTER D.R., WONG M., *The role of mechanical loading histories in the development of diarthrodial joints*, J. Orthop. Res., 1988, 6, 804–816.

[14] CARTER D.R., WONG M., *Modelling cartilage mechanobiology*, Phil. Trans. R. Soc. Lond B, 2003, 358, 1461–1471.

[15] WONG M., CARTER D.R., *A theoretical model of endochondral ossification and bone architectural construction in long bone ontogeny*, Anat. Embryol., 1990, 181, 523–532.

[16] STEVENS S.S., BEAUPRÉ G.S., CARTER D.R., *Computer model of endochondral growth and ossification in long bones: biological and mechanobiological influences*, J. Orthop. Res., 1999, 17, 646–653.

[17] COHEN B., LAI W.M., MOV V.C., *A transversly isotropic biphasic model for unconfined compression of the growth plate and chondroepiphysis*, J. Biomech. Eng., 1998, 120 (4), 491–496.

[18] TANCK E., VAN DRIEL W.D., HAGEN J.W., BURGER E.H., BLANKEVOORT L., HUISKES R., *Why does intermittent hydrostatic pressure enhance the mineralization process in fetal cartilage?* J. Biomech., 1999, 32, 153–161.

[19] PAWLIKOWSKI M., KLASZTORNY M., SKALSKI K., *Studies on constitutive equation that models bone tissue*, Acta Bioeng. Biomech., 2008, 10, 39–47.

[20] MINSTER J., *Modelling of viscoelastic deformation of cortical bone tissue*, Acta Bioeng. Biomech., 2003, 5, 11–21.

[21] SYLVESTRE P.L., VILLEMURE I., AUBON C.E., *Finite element modeling of the growth plate in a detailed spine model*, Med. Bio. Eng. Comput., 2007, 45, 977–988.

[22] LIN H., AUBIN C.E., PARENT S., *Mechanobiological bone growth: comparative analysis of two biomechanical modeling approaches*, Mech. Biol. Eng. Comput., 2009, 47, 357–366.

[23] SHEFELBINE S.J., CARTER D.R., *Mechanobiological predictions of femoral anteversion in cerebral palsy*, Ann. Biomed. Eng., 2004, 32, 297–305.

[24] RIBBLE T.G., SANTARE M.H., MILLER F., *Stresses in the growth plate of the developing proximal femur*, J. Appl. Biomech., 2001, 17, 129–141.

[25] SHEFELBINE S.J, TARDIEU C., CARTER D.R., *Development of the femoral bicondylarangle in hominid bipedalism*, Bone, 2002, 30, No. 5, 765–770.

[26] SHEFELBINE S.J., CARTER D.R., *Mechanobiological predictions of growth front morphology in developmental hip dysplasia*, J. Orthop. Res., 2004, 22, 346–352.

[27] BATHE K.J., *Finite Elements Procedures*, Prentice–Hall, Englewood Cliffs, 1996.

[28] WONG M., CARTER D.R., *Mechanical stress and morphogenetic endochondral ossification of the sternum*, J. Bone Joint Surg. Am., 1988, 70, 992–1000.

[29] VILLEMURE I., CLOUTIER L., MATYAS J.R., DUNCAN N.A., *Non-uniform strain distribution within rat cartilaginous growth plate under uniaxial compression*, J. Biomech., 2007, 40, 149–156.

[30] NOMURA S., TAKANO-YAMAMOTO T., *Molecular events caused by mechanical stress in bone*, Matrix Biology, 2000, 19, 91–96.

[31] PRENDERGAST P.J., KELLY D.J., MCGARRY J.G., *Lecture notes on modelling of the biomechanical behaviour of cells*, Advanced Course on Modelling in Biomechanics MiB'03, IPPT, Warsaw, 2003.

[32] UEKI M., TANAKA N., TANIMOTO K., NISHIO C., HONDA N., LIN Y.Y., TANNE Y., OHKUMA S., KAMIYA T., TANAKA E., TANNE K., *The effect of mechanical loading on the metabolism of growth plate chondrocytes*, Ann. Biomed. Eng., 2008, 36, No. 5, 793–800.